Supporting Information (SI)

Materials and Methods

Protein expression and purification

The cDNAs of mouse Sdk1 $Ig_{1\sim4}$ (residues 1-458) and Sdk2 $Ig_{1\sim4}$ (residues 1-402) were subcloned into pFastBac1 (Invitrogen) vector with a 6xHis tag at the C-terminus, respectively, and the recombinant baculoviruses (Bac-to-Bac) were generated following the instruction form Invitrogen. Hi5 cells were infected and cultured in ESF921 medium (Expression Systems) for protein expression. Supernatants of the target proteins were collected after 72 hrs and loaded onto a Ni-NTA column (Qiagen) equilibrated with 10 column volumes of the equilibrating buffer (50 mM Tris, 150 mM NaCl, 8mM imidazole, pH 8.0). The target proteins were eluted with buffer (50 mM Tris,150 mM NaCl, 250 mM imidazole, pH 8.0) and further purified by a HiLoad 16/600 Superdex 200 pg gel filtration column (GE Healthcare) with TBS buffer (50 mM Tris,150 mM NaCl, pH 8.0). Chicken ovalbumin (Sangon Biotech, Shanghai) and human DEC205/CD205 ectodomain (lab expressed) were used as SEC standards. For selenomethionyl proteins (SeMet protein), Hi5 cells were grown in ESF921 medium (Expression Systems). After 16 hrs of infection, cells were spun down at 800 rpm for 5 mins and the cell pellet was resuspended in methionine-deficient ΔESF921 medium (Expression Systems) and grown for 5 hrs. L-selenomethionine (Affymetrix) was added into the methionine-free media, and cells were grown for 48 hrs before collection.

The constructs of mouse Sdk1, including Sdk1 $Ig_{1\sim4}$ (residues 1-458), Sdk1

www.pnas.org/cgi/doi/10.1073/pnas.1801810115

$Ig_{1\sim6}$ (residues 1-646), $FnIII_{1\sim6}$ (residues 645-1259), $FnIII_{7\sim13}$ (residues 1254-1970), $FnIII_{1\sim13}$ (residues 645-1970), Sdk1 ectodomain (residues 1-1970) and the constructs of mouse Sdk2, including Sdk2 $Ig_{1\sim4}$ (residues 1-402), Sdk2 $Ig_{1\sim6}$ (residues 1-610), $FnIII_{1\sim6}$ (residues 589-1203), $FnIII_{7\sim13}$ (residues 1198-1914), $FnIII_{1\sim13}$(residues 589-1914), and Sdk2 ectodomain (residues 1-1914), were cloned into the pTT5 vector with a 6xHis tag at the C-terminus. Proteins were transiently expressed with PEI (Polysciences) in HEK293F cells cultured in HEK293 FreeStyle media (Invitrogen). The supernatants were collected after 6 days, and the target proteins were purified similarly as described above.

Crystallization and structural determination

Native protein of Sdk1 $Ig_{1\sim4}$ and selenomethionyl protein of Sdk1 $Ig_{1\sim4}$ (SeMet Sdk1 $Ig_{1\sim4}$) were concentrated to ~16 mg/ml in storage buffer (5 mM Tris, 50mM NaCl, pH 7.4) for crystallization. Native protein of Sdk2 $Ig_{1\sim4}$ was concentrated to ~11 mg/ml in storage buffer for crystallization. Crystallization screening was performed using the hanging drop vapor diffusion method at 20 °C by mixing an equal volume (0.5 μl) of protein solution and reservoir solution. Crystals of native and selenomethionyl Sdk1 $Ig_{1\sim4}$ were grown from the drop with the reservoir solution containing 0.1 M Tris (pH 8.0), 30 % PEG 400. Crystals of native Sdk2 $Ig_{1\sim4}$ were grown from the drop with the reservoir solution containing 0.1 M Bis-Tris (pH 5.5), 25 % PEG 3350, 0.2M magnesium chloride hexahydrate. The diffraction data sets were collected at BL17U of the Shanghai Synchrotron Radiation Facility and BL19U1 of the National Facility for Protein Science in Shanghai, and processed with

HKL2000 (Otwinowski and Minor, 1997). Selenomethionyl crystals of Sdk1 $Ig_{1\sim4}$ were prepared for SAD data collection, which diffracted to 2.6 Å with space group P41212 and cell dimension (123.35, 123.35, 57.99, 90.00, 90.00, 90.00). The structure of SeMet-labeled Sdk1 $Ig_{1\sim4}$ crystals was determined using AutoSol in Phenix program suite (Adams et al., 2010) and utilized as a search model for the molecular replacement of the native Sdk1 $Ig_{1\sim4}$ crystals which diffracted to higher resolution. The structure of native Sdk2-$Ig_{1\sim4}$ was solved by molecular replacement using the structure of Sdk1-$Ig_{1\sim4}$ as a search model. Phenix program suite was also used for structural refinement and the program Coot was used for models building (Emsley and Cowtan, 2004). Structural views were generated using pymol (http://www.pymol.org). The diffraction data and refinement statistics are summarized in Table S1.

Negative stain EM

Purified mouse Sdk1 ectodomain and Sdk2 ectodomain were adsorbed to the glow-discharged carbon-coated copper grids and stained with 0.75% (w/v) uranyl formate. The samples were imaged under a Tecnai T12 electron microscope operated at 120 kV. Images were recorded at a nominal magnification of 67,000x using a 4k x 4k Eagle CCD camera with a pixel size of 1.74 Å per pixel. For 2D averaging analysis, 14 particles of the head of Sdk1 dimer and 12 particles of the head of Sdk2 dimer were selected, respectively and used to generate 2D averaging views using EMAN2 software (Tang et al., 2007).

Confocal microscopy

For cell adhesion assays, full-length mouse Sdk1 cDNA (residues 1-2193) and full-length mouse Sdk2 cDNA (residues 1-2176) were cloned into the pTT5 vector using one step cloning kit (Vazyme). EGFP sequence was inserted between the C-terminal end of the ectodomain and the transmembrane domain of Sdk1 and Sdk2, respectively. Cell adhesion assays were performed with HEK293F cells cultured in HEK293 FreeStyle medium (Invitrogen) at 37 °C, 5% CO2, and 120 rpm. After 48 hrs of transfection, the cells were incubated at 95 rpm for 2 hrs, and then plated on coverslips coated with 1 mM poly-L-Lysine, 10 mM $NaHCO_3$ in PBS and incubated overnight. All images were then acquired using a confocal microscope Leica TCS SP8 with a 100x oil immersion lens.

Liposome pull-down assay

Dioleoylphosphatidylcholine (DOPC, PC) (Avanti Lipids) was dried by air-flow in a test tube and suspended in hydration buffer (150 mM NaCl, 50 mM Tris pH 7.4). The lipid suspension was extruded through a 200 nm membrane filter with a Mini-Extruder (Avanti Lipids) to generate liposomes for pull-down assays. Roughly 100 nmol liposomes were incubated with 200 ng of each protein sample for 1 hr at room temperature, and centrifuged at 16,000 x g for 30 min at 22 °C. The lipid pellets were washed twice with washing buffer (150 mM NaCl, 50 mM Tris pH 7.4). Then the supernatant (W) and the pellet (P) were loaded onto SDSPAGE followed by western blot detection using mouse anti-His antibody. Immunoreactive bands were detected with goat anti-mouse IgG conjugated with horseradish peroxidase (1:1000) and developed using the diaminobenzidine detection method.

Cryo-electron tomography

Dioleoylphosphatidylcholine (DOPC) and 1,2-dioleoyl-snglycero-3- [(N-(5-amino-1 carboxypentyl) iminodiacetic acid) succinyl] (DOGS-NTA) (Avanti Lipids) were used for liposome preparation. Briefly, a mixture of 2.5 mmol DOPC and 0.5 mmol DOGS-NTA in $CHCl_3$ was evaporated under nitrogen flow and hydrated with 0.2 ml binding buffer (150 mM NaCl, 50 mM Tris pH 7.4) for 1 hr. Then the suspension was passed through a 200 nm membrane filter with a Mini-Extruder (Avanti Lipids). 20 μl liposomes were incubated with about 100 ng his-tagged Sdk1 ectodomain proteins for 1 hr. The liposomes were also mixed with 10 nm colloidal gold particles (Sigma) as fiducial markers for image alignment, and then loaded onto glow-discharged lacy carbon grids (Ted Pella, Inc.) followed by vitrification in liquid ethane using a Vitrobot (FEI). Tilt series were collected between ±65 degree at 1.5 degree increment with an Falcon II direct electron detector using Xplore3D software (FEI) on a Titan Krios electron microscope (FEI) operating at 300 kV. Images were acquired under low-dose conditions with a total dose of ~100 e-/Å ^{2} at a nominal magnification of 37,000x, which corresponds to a pixel size of 2.8 Å. The defocus values were set to 4~5 μm. 3D reconstructions were generated by the simultaneous reconstruction technique (SIRT) implemented in IMOD (Kremer et al., 1996).

Fluorescence microscopy

HEK293 cells were transfected by the full length Sdk1-GFP, the full length Sdk2-GFP, Sdk1 $Ig_{1\sim6}$-GFP and Sdk2 $Ig_{1\sim6}$-GFP, respectively. After 24 hrs of

transfection, the cells were resuspended in HEK293 Freestyle medium (Invitrogen) and grown overnight on a shaker at 100 rpm. An EM finder grid was put on the top of a 3 mm sapphire disc (McDonald et al., 2010), and the pattern on the finder grid could be printed on the sapphire disc by carbon evaporation and became recognizable under light microscope. HEK293F cells expressing Sdk1-GFP, Sdk2-GFP, Sdk1 $Ig_{1\sim6}$-GFP, Sdk2 $Ig_{1\sim6}$-GFP were attached on the sapphire discs coated with 1mM poly-L-lysine (Sigma) and incubated for 2 hrs at 37 °C. Then fluorescence images of the cells were recorded by an Olympus IX inverted microscope to locate the areas containing cell-cell contacts.

High pressure freezing and freeze substitution

A sapphire disc was placed on a flat aluminum planchette with cells facing up, another aluminum planchette with 40 μm depth inner space was used as a cover, and the space between the two planchettes was filled with hexadecane. The sandwich was placed on the specimen holder and frozen in a Wohlwend HPF Compact 2 high-pressure freezer (M. Wohlwend GmbH, Sennwald, Switzerland) under a pressure of 2100 bar. The frozen specimens were transferred into cryo-tubes containing fixative (with 1% osmium tetroxide and 0.1% uranyl acetate in acetone) at liquid nitrogen temperature followed by freeze substitution and plastic embedding (McDonald, 2014). The finder grid pattern and the area of interest could be identified on the surface of the resin block, and the surrounding regions were trimmed off with a razor blade (Note: some of the cells might be lost during HPF, but this would not affect the location of the remaining cells.). To check the location of cells, a couple of

semi-thin sections of 500 nm thickness were cut and inspected under a light microscope after staining with 0.5% (w/v) toluidine blue (Tanaka et al., 2012) to find target cells. Then serial thin sections (100 nm thickness) were prepared from the remaining block and collected onto formvar-coated copper grids. The sections were stained with 3% uranyl acetate in 70% methanol and 30% water for 7 mins at 4 °C, followed by staining with lead citrate for 10 mins at room temperature. The stained sections were loaded onto at a FEI Tecnai G2 (120kV) electron microscope for imaging.

Immuno-labeling electron microscopy

HEK293T cells cultured on sapphire discs were transfected with Sdk1-GFP and Sdk2-GFP, respectively. After 48 hrs, the transfected cells were examined under a fluorescence microscope and then fixed by HPF and substituted in acetone with 0.2% uranyl acetate following the substitution protocol described above. Then the cells were infiltrated with 25%, 50%, 75%, and pure epon812 resin respectively. After embedding, the samples were polymerized at 60 °C for 24 hrs. The blocks were trimmed and thin sectioned with thickness of 100 nm. A serial thin sections were collected on formvar-coated nickel grids and blocked in 0.01M PBS containing 1%BSA, 0.05% TritonX-100 and 0.05% Tween 20 for 10min. The sections were labeled by anti-GFP antibody diluted in 0.01M PBS containing 1%BSA and 0.05% Tween 20 for 2 hrs at room temperature. After washing with 0.01M PBS six times (2 min each), the sections were labeled by the 10 nm gold conjugated secondary antibody diluted in 0.01M PBS containing 1%BSA and 0.05% Tween 20 for 1 hr at

room temperature. Then the sections were washed with 0.01M PBS six times and distilled water four times (2 min each) and stained with 3% uranyl acetate in 70% methanol and 30% water for 7 min at 4 °C, then stained with lead citrate for 3 min at room temperature and loaded onto a FEI (Tecnai G2 Spirit 120kV) electron microscope for imaging. (Note: since no osmium tetroxide was added during fixation for immuno-labeling, the membrane preservation was not as good as regular fixation.)

Electron tomography

Thin sections prepared by the HPF-FS method were loaded onto a FEI Tecnai G2 electron microscope (120 kV) for imaging and tilt series collection. Single-axis tilt series were collected between -60° to +60° with 1.5 degree angular increment at a magnification of 67,000x using Xplore3D software (FEI). Tomograms were calculated using IMOD (Kremer et al., 1996). Sub-tomogram volume truncation and iso-surface rendering were carried out using IMOD. Crystal structure of Sdk1 $Ig_{1\sim5}$ (PDB entry: 5k6w) were fitted into the tomographic density manually using UCSF chimera (Goddard et al., 2007).

Supplementary Figure 1

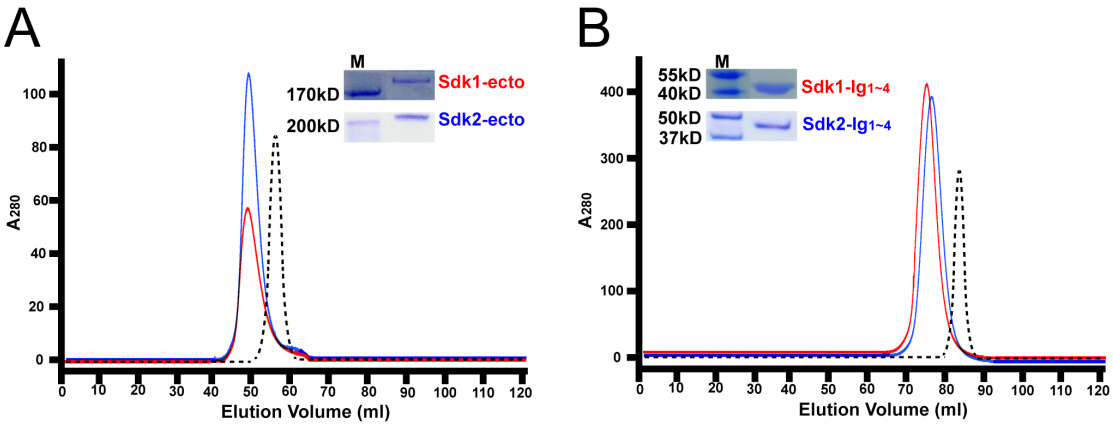

Figure S1 Expression and purification of Sdk1 and Sdk2.

(A) Size-exclusion chromatography of Sdk1 ectodomain (red) and Sdk2 ectodomain (blue). The eluates are analyzed by SDS-PAGE (inset). The elution profile of a protein with similar molecular weight (human DEC205/CD205 ectodomain, MW ~200kD) is shown as a control (black dashed line).

(B) Size-exclusion chromatography of Sdk1 $Ig_{1\sim4}$ (red) and Sdk2 $Ig_{1\sim4}$ (blue). The eluates are analyzed by SDS-PAGE (inset). The elution profile of a protein with similar molecular weight (chicken ovalbumin, MW ~44kD) is shown as a control (black dashed line).

Supplementary Figure 2

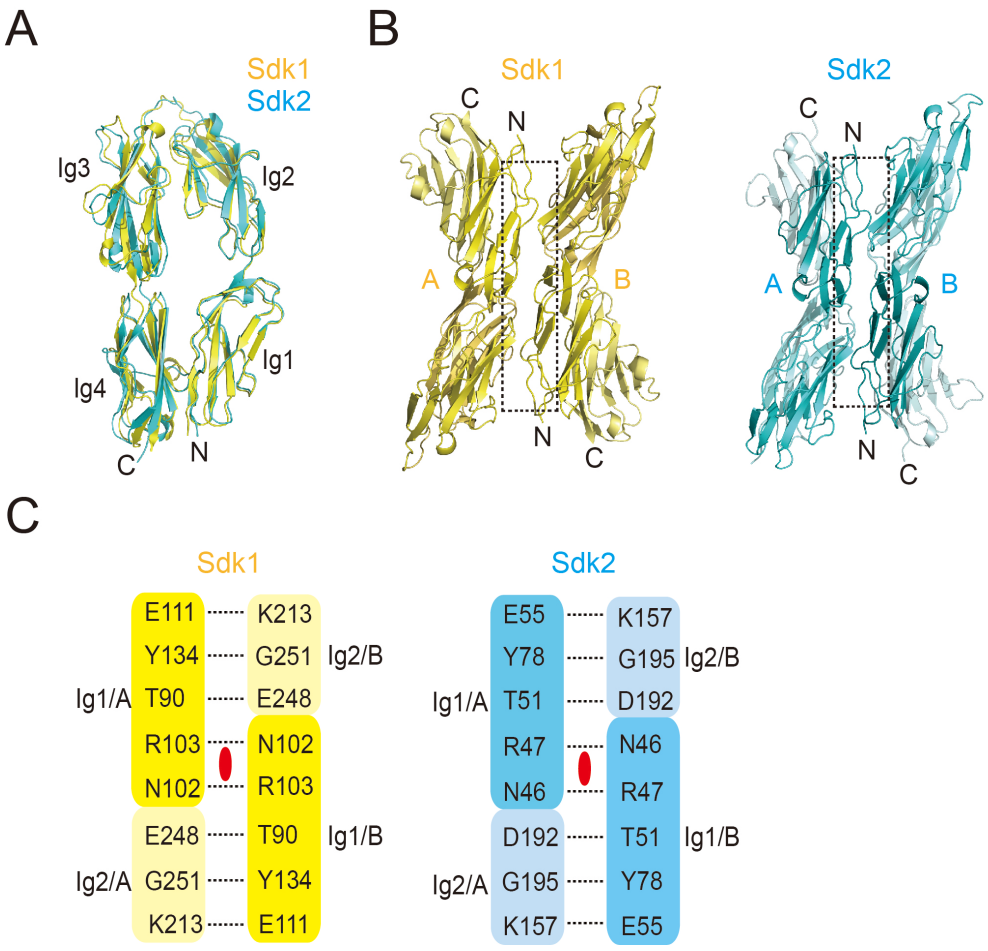

Figure S2 Crystal structures of Sdk1 $Ig_{1\sim4}$ and Sdk2 $Ig_{1\sim4}$.

(A) The four N-terminal Ig-like domains of Sdk1 (yellow) and Sdk2 (cyan) form a horseshoe-shaped conformation.

(B) Ribbon diagrams of Sdk1 $Ig_{1\sim4}$ dimer (left) and Sdk2 $Ig_{1\sim4}$ dimer (right). The dimeric interfaces are indicated by the black dashed boxes.

(C) Schematic diagrams of the interacting residues forming the homophilic dimerization interfaces of Sdk1 (left) and Sdk2 (right). The red ovals indicate the dimeric 2-fold axes. Residue numbering includes the N-terminal signal sequence of Sdk1 or Sdk2.

Supplementary Figure 3

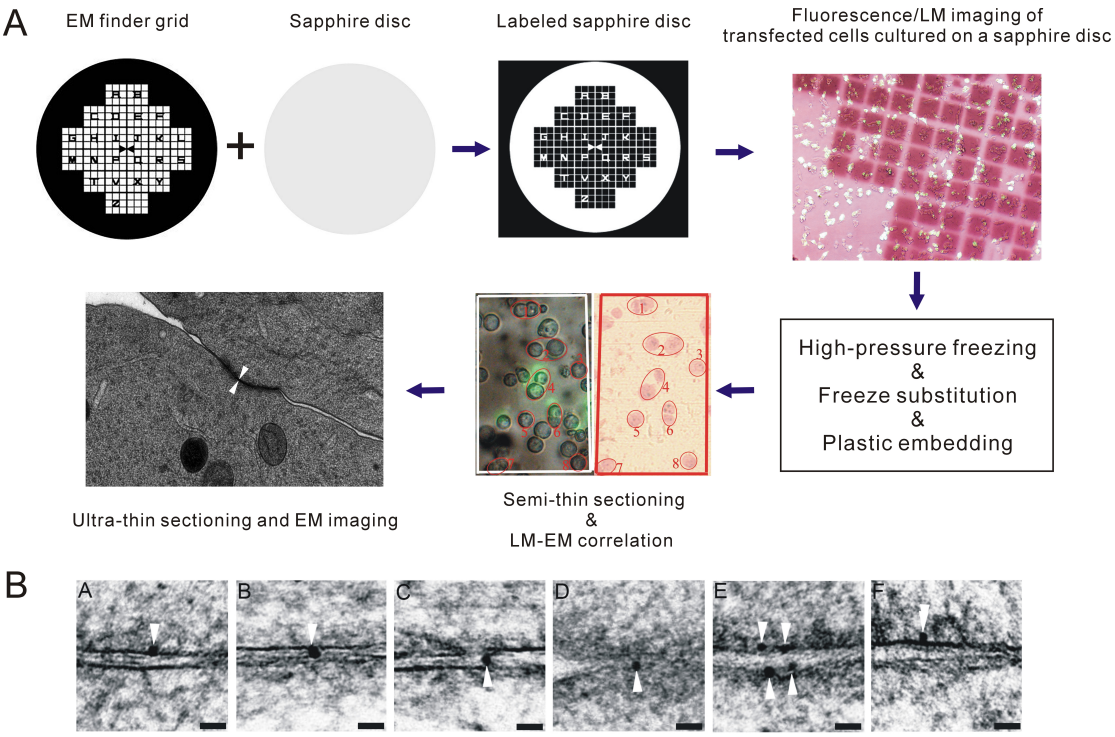

Figure S3

(A) A flowchart of correlative light-electron microscopy sample preparation.

(B) The immune-gold (white arrowheads) labeling of Sdk1 (A-C) or Sdk2 (D-F) molecules at cell adhesion interfaces (bar, 20 nm).

Supplementary Figure 4

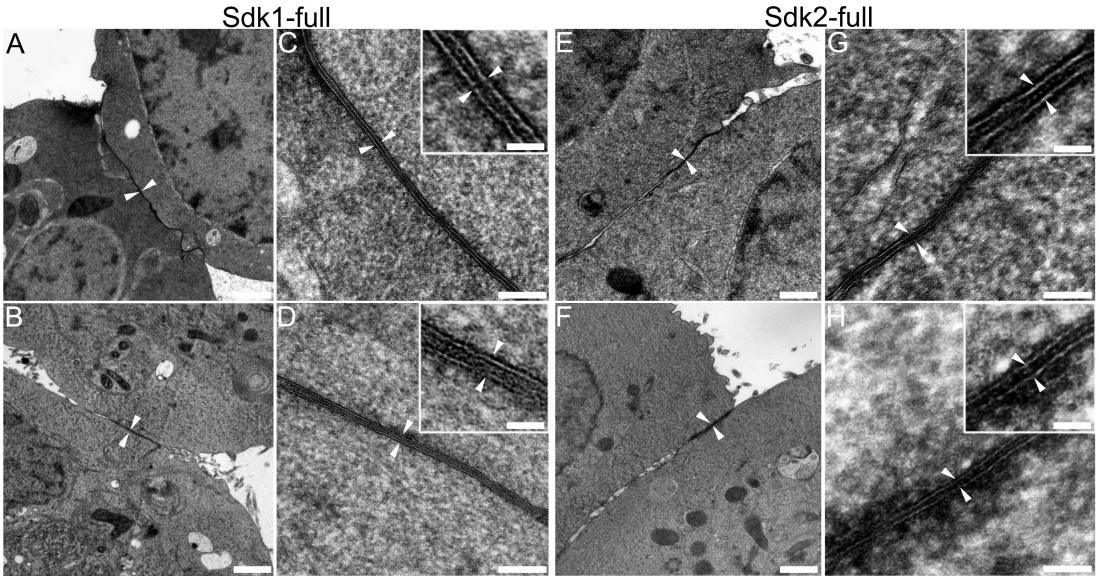

Figure S4 EM images of thin sections showing the cell adhesion interfaces mediated by Sdk1 and Sdk2, respectively.

(A-B) Electron micrographs of cell adhesion interfaces (white arrowheads) mediated by the full length Sdk1 at low magnification (bar, 1μm).

(C-D) Electron micrographs of cell adhesion interfaces (white arrowheads) mediated by the full length Sdk1 at medium (bar, 50 nm) and high (inset; bar, 25 nm) magnifications.

(E-F) Electron micrographs of cell adhesion interfaces (white arrowheads) mediated by the full length Sdk2 at low magnification (bar, 1μm).

(G-H) Electron micrographs of cell adhesion interfaces (white arrowheads) mediated by the full length Sdk2 at medium (bar, 50 nm) and high (inset; bar, 25 nm) magnification.

Supplementary Figure 5

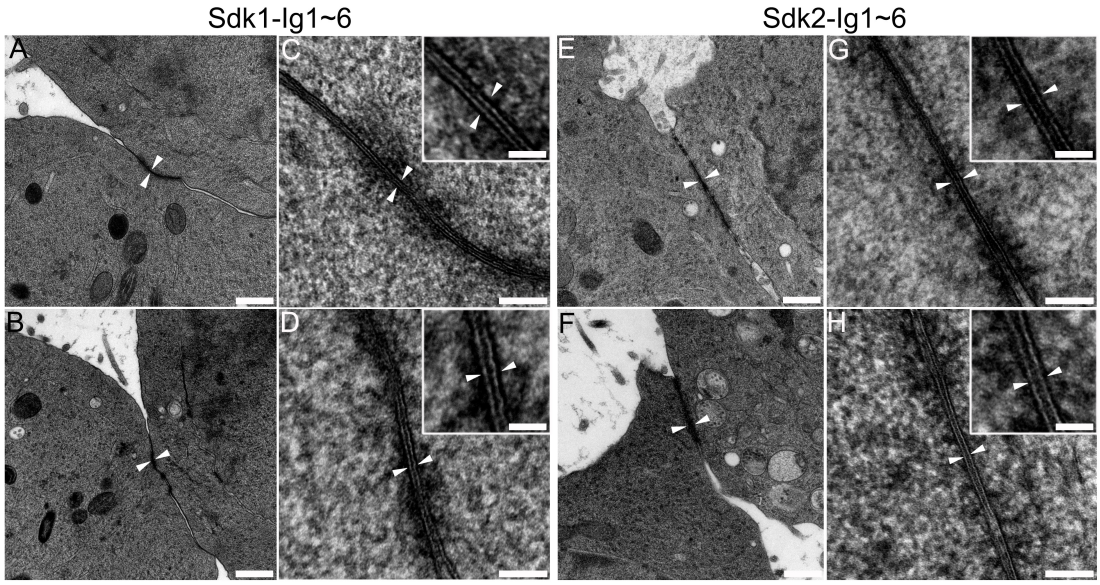

Figure S5 EM images of thin sections showing the cell adhesion interfaces mediated by Sdk1 $Ig_{1\sim6}$ and Sdk2 $Ig_{1\sim6,}$ respectively.

(A-B) Electron micrographs of cell adhesion interfaces (white arrowheads) mediated by the Sdk1 $Ig_{1\sim6}$ at low magnification (bar, 1μm).

(C-D) Electron micrographs of cell adhesion interfaces (white arrowheads) mediated by the Sdk1 $Ig_{1\sim6}$ at medium (bar, 50 nm) and high (inset; bar, 25 nm) magnification.

(E-F) Electron micrographs of cell adhesion interfaces (white arrowheads) mediated by the Sdk2 $Ig_{1\sim6}$ at low magnification (bar, 1μm).

(G-H) Electron micrographs of cell adhesion interfaces (white arrowheads) mediated by the Sdk2 $Ig_{1\sim6}$ at medium (bar, 50 nm) and high (inset; bar, 25 nm) magnification.

Supplementary Figure 6

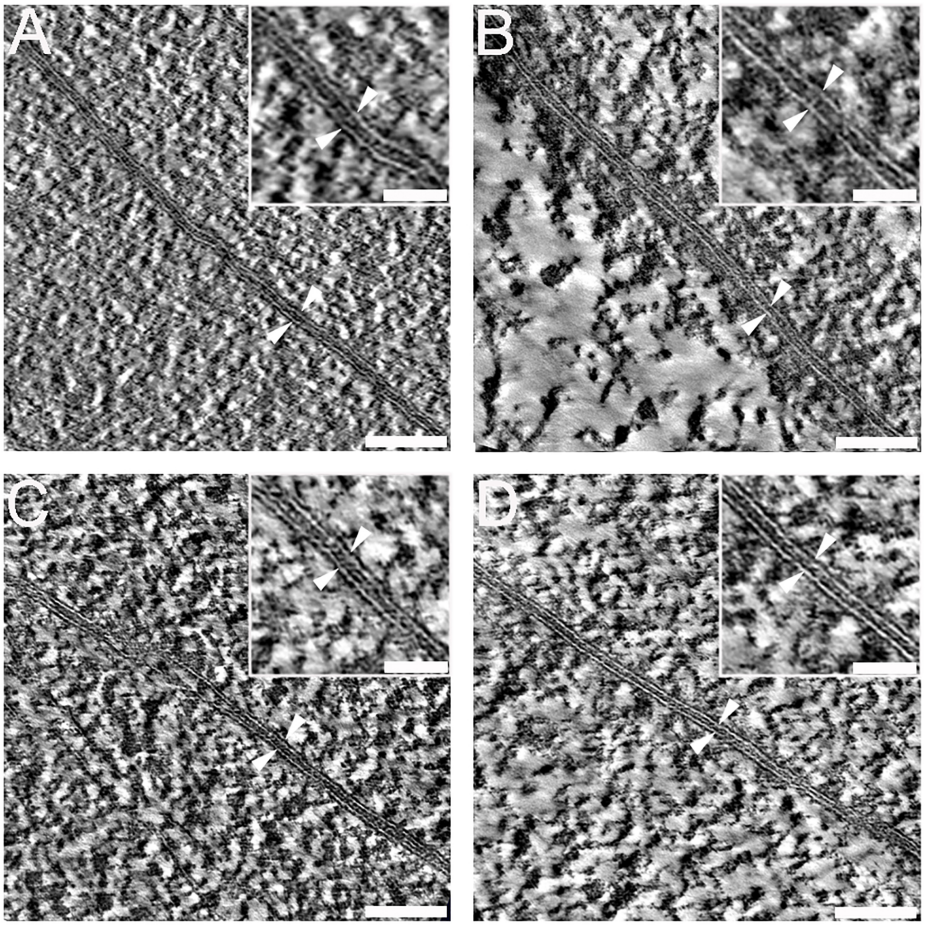

Figure S6 Tomograms of cell adhesion interfaces formed by Sdk molecules.

Tomographic slices of cell adhesion interfaces (white arrowheads) formed by Sdk1 (A), Sdk2 (B), Sdk1 $Ig_{1\sim6}$ (C) and Sdk2 $Ig_{1\sim6}$ (D) are shown at low (bar, 50 nm) and high (insets; bar, 35 nm) magnifications.

Supplementary Table S1

Table 1. Data collection and refinement statistics

	Native Sdk1-Ig$_{1\sim4}$	Native Sdk2-Ig$_{1\sim4}$
Data Collection		
Beamline	SSRF BL17U1	SSRF BL17U1
Wavelength (Å)	0.979	0.979
Space group	P21 21 21	P21 21 21
Unit cell a, b, c (Å)	63.85,118.06,122.84	82.35,86.80,108.55
Unit cell α, β, γ (º)	90.00, 90.00, 90.00	90.00, 90.00, 90.00
Resolution (Å) *	30.0-1.55 (1.61-1.55)	30.0-2.40 (2.49-2.40)
Completeness (%)*	97.1 (94.8)	97.8 (93.6)
Redundancy*	5.3 (3.5)	4.7 (3.1)
I/sigma(I) *	10.1 (2.6)	22.2 (2.7)
R_{merge}*	0.118 (0.38)	0.065 (0.44)
Refinement Statistics		
Resolution (Å)	29.5-1.55	28.8-2.39
No. of reflections	131095	30490
R_{work} / R_{free}	20.4/24.7	22.8/28.4
Number of atoms	5862	5870
Protein residues	752	741
B-factor	29.8	62.4
R. m. s. deviations		
Bond lengths (Å)	0.006	0.013
Bond angles (º)	1.10	1.52
Ramachandran Statistics (%)		
Most favored	98	96
Allowed	2	4
Outliers	0	0

* Numbers in the brackets are for the highest resolution shell.

References

Adams, P.D., Afonine, P.V., Bunkoczi, G., Chen, V.B., Davis, I.W., Echols, N., Headd, J.J., Hung, L.W., Kapral, G.J., Grosse-Kunstleve, R.W.*, et al.* (2010). PHENIX: a comprehensive Python-based system for macromolecular structure solution. Acta Crystallogr D *66*, 213-221.

Emsley, P., and Cowtan, K. (2004). Coot: model-building tools for molecular graphics. Acta Crystallogr D *60*, 2126-2132.

Goddard, T.D., Huang, C.C., and Ferrin, T.E. (2007). Visualizing density maps with UCSF Chimera.

Journal of structural biology *157*, 281-287.
Kremer, J.R., Mastronarde, D.N., and McIntosh, J.R. (1996). Computer visualization of three-dimensional image data using IMOD. Journal of structural biology *116*, 71-76.
McDonald, K., Schwarz, H., Muller-Reichert, T., Webb, R., Buser, C., and Morphew, M. (2010). "Tips and tricks" for high-pressure freezing of model systems. Methods Cell Biol *96*, 671-693.
McDonald, K.L. (2014). Out with the old and in with the new: rapid specimen preparation procedures for electron microscopy of sectioned biological material. Protoplasma *251*, 429-448.
Otwinowski, Z., and Minor, W. (1997). Processing of X-ray diffraction data collected in oscillation mode. Macromolecular Crystallography, Pt A *276*, 307-326.
Tanaka, H., Miyazaki, N., Matoba, K., Nogi, T., Iwasaki, K., and Takagi, J. (2012). Higher-order architecture of cell adhesion mediated by polymorphic synaptic adhesion molecules neurexin and neuroligin. Cell Rep *2*, 101-110.
Tang, G., Peng, L., Baldwin, P.R., Mann, D.S., Jiang, W., Rees, I., and Ludtke, S.J. (2007). EMAN2: an extensible image processing suite for electron microscopy. Journal of structural biology *157*, 38-46.